IEICE TRANS. FUNDAMENTALS, VOL.E102–A, NO.3 MARCH 2019

PAPER

Induced Synchronization of Chaos–Chaos Intermittency Maintaining Asynchronous State of Chaotic Orbits by External Feedback Signals

Sou NOBUKAWA[†a)], **Haruhiko NISHIMURA**[††], ***Members***, **Teruya YAMANISHI**[†††], ***Nonmember***, ***and*** **Hirotaka DOHO**[††,††††], ***Member***

SUMMARY It is well-known that chaos synchronization in coupled chaotic systems arises from conditions with specific coupling, such as complete, phase, and generalized synchronization. Recently, several methods for controlling this chaos synchronization using a nonlinear feedback controller have been proposed. In this study, we applied a proposed reducing range of orbit feedback method to coupled cubic maps in order to control synchronization of chaos–chaos intermittency. By evaluating the system's behavior and its dependence on the feedback and coupling strength, we confirmed that synchronization of chaos–chaos intermittency could be induced using this nonlinear feedback controller, despite the fact that the asynchronous state within a unilateral attractor is maintained. In particular, the degree of synchronization is high at the edge between the chaos–chaos intermittency parameter region for feedback strength and the non-chaos–chaos intermittency region. These characteristics are largely maintained on large-scale coupled cubic maps.

key words: *synchronization, chaos-chaos intermittency, control*

1. Introduction

In non-linear systems, fluctuating activity induces divergent synchronization phenomena such as synchronization transitions and chimera states [1]–[6]. Stochastic resonance is an example one of these synchronization phenomena in which the responsiveness to a weak (under barrier) signal in a nonlinear system is enhanced by noise when the system satisfies several specific criteria related to the form of the barrier/threshold, noise sources, and the weakness of the input signal [7]–[9].

Chaotic oscillations have the characteristics of synchronization with external input signals or with other oscillations in a network consisting of chaotic oscillations [10]. In the former type of synchronization, chaotic processes cause a phenomenon similar to stochastic resonance with a deterministic fluctuating activity instead of stochastic noise, known as chaotic resonance [11]. Chaotic resonance was first discovered in systems with chaos–chaos intermittency (CCI), which is the chaotic state in which the chaotic orbit goes back and forth among the separated regions, as typified in a one-dimensional cubic map and a Chua circuit [12]–[16]. In these systems, chaotic resonance is produced by synchronization between the CCI and a weak input signal near the bifurcation point of the merging attractor [11]. Furthermore, it was reported that chaotic resonance arises in neural systems and has a higher sensitivity than stochastic resonance [17]–[22]. However, few studies have focused on engineering applications based on chaotic resonance despite the numerous applications of stochastic resonance such as wearable devices that enhance human tactile sensitivity [23], [24]. This could be because the chaotic state is induced by the adjustment of internal parameters of the system. In many cases, the external control of these parameters is difficult, particularly in the case of biological systems. To overcome this difficulty, we proposed a method for controlling chaotic resonance based on the external feedback signal approach discussed in our previous work [25]. In particular, the proposed feedback signal reduces the range of orbit by adjusting the local maximum and minimum values of the map function and controls merging of the attractor and the CCI frequency, instead of adjusting the internal parameters. This is called the reducing the range of orbit (RRO) feedback method in this study. Hence, the synchronization of CCI against a weak external signal arises at an appropriate feedback strength.

In the latter type of synchronization among chaotic oscillators, several kinds of chaos synchronization [10] have been widely observed under conditions with specific coupled forms, such as complete [26]–[28], phase [29], and generalized synchronization [30]. Several methods for controlling chaos synchronization based on a nonlinear feedback controller have been proposed [31]–[34]. In particular, these non-linear controllers utilize Lyapunov stability [31], [32], active control [33] and converse Lyapunov theories [34]. Out of all these available methods, CCI synchronization was induced in two coupled cubic maps using a RRO feedback signal in our previous work [35]. However, the characteristics of synchronization in large-scale coupled oscillators and the relationship between CCI synchronization and the stability of chaotic orbits/synchronization have not been investigated.

In this study, we show that CCI synchronization can be

Manuscript received August 21, 2018.
Manuscript revised November 6, 2018.

[†]The author is with Department of Computer Science, Chiba Institute of Technology, Narashino-shi, 275-0016 Japan.
[††]The authors are with Graduate School of Applied Informatics, University of Hyogo, Kobe-shi, 650-8588 Japan.
[†††]The author is with Department of Management Information Science, Fukui University of Technology, Fukui-shi, 910-8505 Japan.
[††††]The author is with Faculty of Education, Teacher Training Division, Kochi University, Kochi-shi, 780-8520 Japan.
a) E-mail: nobukawa@cs.it-chiba.ac.jp
DOI: 10.1587/transfun.E102.A.524

controlled using our RRO feedback method in coupled cubic maps based on our previous work [35]. We then, control the merging of the attractor in coupled cubic maps expanded from two to hundreds of map elements, and the synchronization control was evaluated based on external feedback. Finally, we evaluated the relationship between CCI synchronization and the stability of chaotic orbits/synchronization using the Lyapunov exponent and transverse Lyapunov exponent.

2. Material and Methods

2.1 Cubic Map Model with External Feedback and Coupled Cubic Maps

A one-dimensional cubic map model is a relatively simple model in which CCI occurs, i.e., the chaotic orbit goes back and forth between the positive and negative regions [11]. In this study, RRO feedback $Ku(x)$ is applied to the one-dimensional cubic map model:

$$x(t+1) = F(x(t)) + Ku(x(t)), \tag{1}$$

$$F(x) = (ax - x^3)\exp(-x^2/b), \tag{2}$$

$$u(x) = -(x - x_d)\exp(-(x - x_d)^2/(2\sigma^2)), \tag{3}$$

where K and x_d are the amplitude related to the feedback control intensity and the point dividing each attractor, respectively. The cubic map in Eq. (2) has two symmetric attractor regions, i.e., positive and negative $x(t)$ regions. Therefore, we set $x_d = 0$. The RRO feedback term $Ku(x)$ reduces the absolute values for the local maximum and minimum of $F(x)$. The parameter set $(a = 2.86, b = 10, \sigma = 0.6)$ is used in this study. In the $K = 0$ case, a chaotic orbit of $x(t)$ distributes across the positive and negative x regions.

We use a ring-type network consisting of N cubic maps near a gap junction with strength J:

$$x_i(t+1) = F(x_i(t)) + Ku(x_i(t)) + J(2x_i - x_{i-1} - x_{i+1}) \quad (i = 1, \cdots, N), \tag{4}$$

where the periodic boundary condition is applied in the $i = 1, N$ cases. In Eq. (4), if the ordinal diffusive coupling is set such that $(x_{i-1} + x_{i+1} - 2x_i)$, the cubic maps induce synchronization with opposite phase at a sufficient coupling strength. Therefore, to evaluate synchronization with the coordinate phase, the inverse sign of diffusive coupling is defined.

2.2 Evaluation Index

CCI synchronization was evaluated using the correlation coefficient between $X_i(t)$ and $X_j(t)$ $(i, j = 1, 2, \cdots, N, i \neq j)$, which are binarized time series of $x_i(t)$ and $x_j(t)$ ($X_{i,j}(t) = 1$ in the $x_{i,j}(t) \geq 0$ case, $X_{i,j}(t) = -1$ in the $x_{i,j}(t) < 0$ case) as follows:

$$C(\tau) = \frac{C_{ij}(\tau)}{\sqrt{C_{ii}C_{jj}}} \tag{5}$$

$$C_{ij}(\tau) = \langle (X_i(t+\tau) - \langle X_i \rangle)(X_j(t) - \langle X_j \rangle) \rangle \tag{6}$$

$$C_{ii} = \langle (X_i(t) - \langle X_i \rangle)^2 \rangle \tag{7}$$

$$C_{jj} = \langle (X_j(t) - \langle X_j \rangle)^2 \rangle, \tag{8}$$

where $\langle \cdot \rangle$ denotes the average in t.

To evaluate the chaos in the coupled cubic maps, we use the maximum Lyapunov exponent [36]:

$$\lambda_1 = \frac{1}{\tau_l M}\sum_{k=1}^{M} \ln\left(\frac{|\mathbf{d}^k(t_l = \tau_l)|}{|\mathbf{d}^k(t_l = 0)|}\right). \tag{9}$$

Here, $\mathbf{d}^k(t_l = 0)$ are M the perturbed initial conditions for $\{x_1(t), x_2(t), \cdots, x_N(t)\}$ applied at $t = t_0 + (k-1)\tau_l$, which are given by:

$$\mathbf{d}^{k+1}(t_l = 0) = |\mathbf{d}_0|\frac{\mathbf{d}^k(t_l = \tau_l)}{|\mathbf{d}^k(t_l = \tau_l)|}, \tag{10}$$

where $\mathbf{d}^1(t_l = 0) = \mathbf{d}_0$, ($\mathbf{d}_0$: an initial vector). In addition, $\mathbf{d}^k(t_l = \tau_l)$ indicates the time evolution of the perturbed vector for $t_l \in [0 : \tau_l]$. In this study, we use $\tau_l = 1$ and $\mathbf{d}_0 = 10^{-6}$.

Furthermore, in the case of the coupled cubic maps, the synchronization stability was evaluated from the maximum transverse Lyapunov exponent [10]. To perform this estimation, we utilized a method proposed by Dabrowski [37]. According to this method, the time evolution of the perturbation vector $\mathbf{d_s}^k(t_\perp)$ $(k = 1, 2, \cdots, M)$ from the synchronization manifold during $t_\perp \in [0 : \tau_\perp]$ is calculated. Here, the initial perturbation $\mathbf{d_s}^k(0)$ is applied at $t = t_0 + (k-1)\tau_\perp$. Then, the inner product between the perturbation vector and its temporal derivative is calculated as follows:

$$\lambda_s^k = \frac{\mathbf{d_s}^k(\tau_\perp) \cdot \frac{d\mathbf{d_s}^k(\tau_\perp)}{dt}}{|\mathbf{d_s}^k(\tau_\perp)|^2}, \tag{11}$$

where $\cdot$ indicates the inner product. The maximum transverse Lyapunov exponent is given by

$$\lambda_\perp = \frac{1}{\tau_\perp M}\sum_{k=1}^{M} \lambda_s^k. \tag{12}$$

In this study, $\tau_\perp = 5$ and the initial perturbation amplitude $\mathbf{d_s}^k(0) = 10^{-6}$ are set.

3. Results

3.1 Control Method for Attractor Merging by External Feedback

We consider a control method for separating the merged attractor by applying an external feedback $Ku(x)$. The upper panel of Fig. 1(a) shows the orbit and map in the attractor-merging case. The arrows indicate the attractor switching points, i.e., the attractor switches from the positive region $(x(t) > 0)$ to the negative region $(x(t) < 0)$ at $x(t) \approx 1.7$, whereas the attractor switches from the negative region

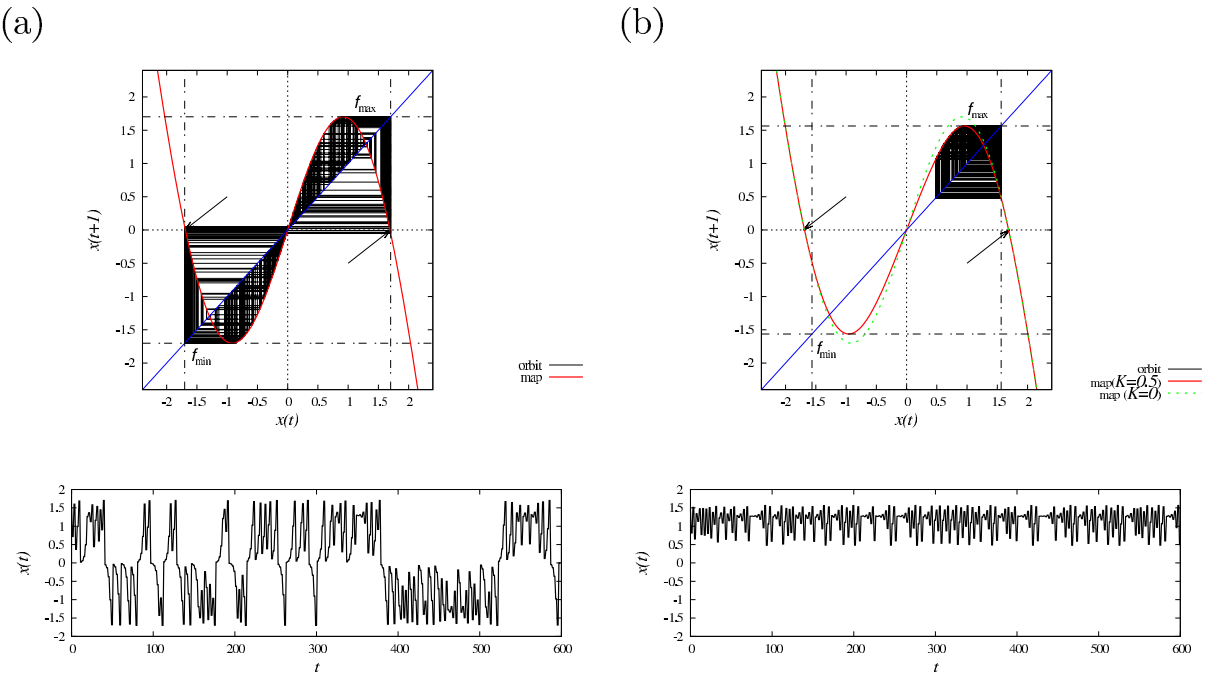

Fig. 1 (a) Return map of the cubic map without a feedback term ($K = 0$) and its orbit (upper panel). Time series of $x(t)$ (lower panel). The arrows indicate the attractor switching points. The dashed lines indicate the local maximum ($f_{\max}$) and minimum ($f_{\min}$) values of the cubic map at $x \approx \pm 0.916$. (b) Return map of the cubic map with the feedback term and its orbit (upper panel). Time series of $x(t)$ (lower panel). These figures are partially modified and quoted from Ref. [25] ($a = 2.86$, $b = 10$, $\sigma = 0.6$).

($x(t) < 0$) to the positive region ($x(t) > 0$) at $x(t) \approx -1.7$. This attractor switching is also observed in the lower part of Fig. 1(a). From this result, we confirm that CCI arises when $F(f_{\max}) < 0$ and $F(f_{\min}) > 0$, where $f_{\max}$, $f_{\min}$, and $F(f_{\max,\min})$ indicate the local maximum and minimum values of the map at $x \approx \pm 0.916$, the intersections of the map function, and the vertical dashed lines, respectively. We adopted the feedback $Ku(x)$ ($K = 0.5$) to suppress CCI. This feedback has the effect of reducing the absolute value of $f_{\max,\min}$. It leads to a break of the conditions $F(f_{\max}) + Ku(f_{\max}) < 0$ and $F(f_{\min}) + Ku(f_{\min}) > 0$ (see Fig. 1(b)). Consequently, as shown in Fig. 1(b), the orbit is confined in the unilateral region corresponding to the region where the initial value $x(0)$ is located (see the solid black line in the upper and lower parts).

3.2 Controlling the Synchronization of CCI by External Feedback

Initially, CCI synchronization was evaluated in the two coupled cubic maps ($N = 2$) given by Eq. (4). Figure 2(a) shows the time series of $x_1(t)$ and $x_2(t)$ at the gap junction $J = 0.05$. When $K = 0.05$, the CCI dynamics in $x_1(t)$ and $x_2(t)$ do not synchronize. Meanwhile, when $K = 0.25$, the CCI frequency decreases and CCI synchronization occurs. At larger values of K ($K = 0.3$), $x_1(t)$ and $x_2(t)$ are trapped in the unilateral attractor region. These temporal expanded figures are presented in Fig. 2(b). The orbit of each element $(x_1(t), x_2(t))$ in the internal unilateral regions does not synchronize, even when CCI synchronization occurs ($K = 0.25$). Figure 3 shows $C(0)$ for the time series of $x_1(t)$ and $x_2(t)$, λ_1, and $\lambda_\perp$ as functions of the gap junction J and feedback strength K. Here, $C(0)$ exhibits a high value ($C(0) \gtrsim 0.7$) at the edge between the CCI and the non-CCI regions. The white region corresponding to $C(0)$ in Fig. 3 represents the non-CCI region, i.e., the $x_{1,2}$ orbits are confined within the unilateral region. The peak values of $C(0)$ increases as J increases. In this region with a large $C(0)$ value, the dynamics exhibit chaos ($\lambda_1 > 0$) and an unstable synchronous state ($\lambda_\perp > 0$). This means that the chaotic dynamics in the unilateral attractor region desynchronizes each other for this weak coupling strength, even if CCI synchronizes.

Secondly, we evaluated control synchronization of the CCI in larger-scale coupled cubic maps. The upper panels in Fig. 4 show the mean value of the correlation coefficient $C(\tau = 0)$ for the time series of $x_i(t)$ and $x_j(t)$ ($i, j = 1, 2, \cdots N, i \neq j$) for all pairs of cubic maps as a function of the gap junction J and feedback strength K. λ_1 as a function of J and K is presented in the lower panels in the figure. Here, $C(0)$, λ_1, and $\lambda_\perp$ exhibit the same tendency as the case of the two coupled cubic maps. That is, for all sizes of coupled cubic maps, $C(0)$ has a large value at the edge between the CCI and non-CCI regions. However, the regions with a large value of $C(0)$ are narrow, and these values decrease as N increases. In addition, the maximum $C(0)$ values are plotted as a function of N with respect to the parameter region for $0 \leq J \leq 0.1$ and $0 \leq K \leq 0.3$ in

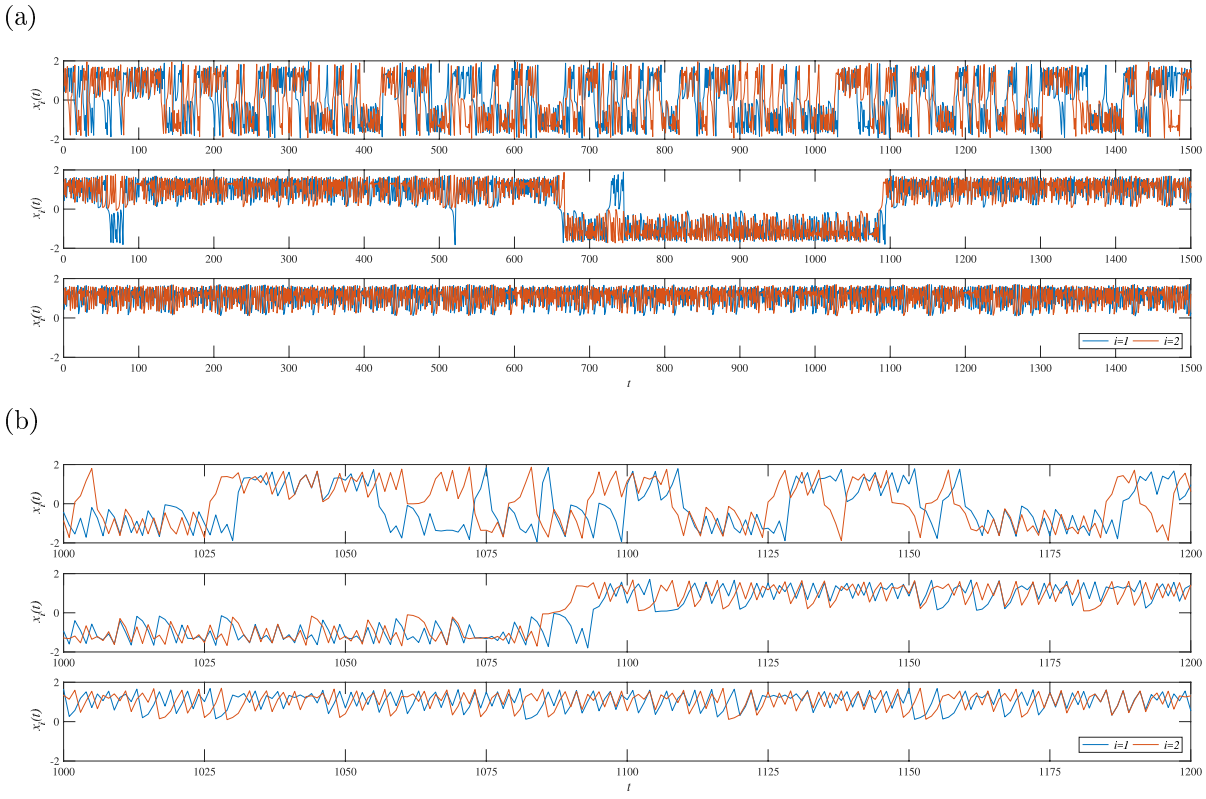

Fig. 2 (a) Time series of $x_{1,2}(t)$ in $K = 0.05$ (top), 0.25 (middle), and 0.3 (bottom). (b) Temporally expanded figures of the time series in (a) ($a = 2.86$, $b = 10$, $\sigma = 0.6$, $J = 0.05$, $N = 2$).

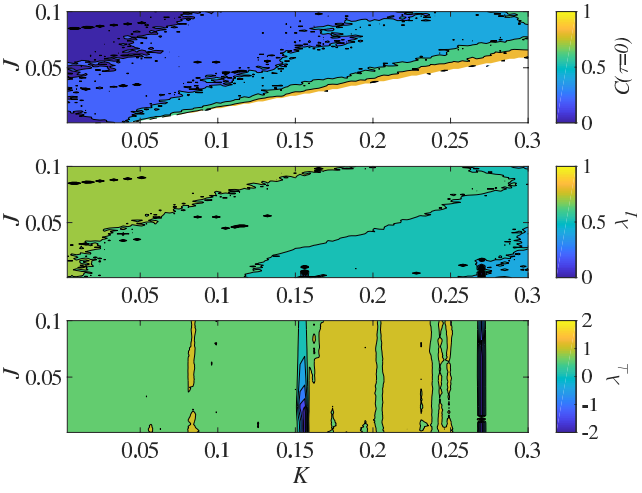

Fig. 3 Correlation coefficient $C(\tau = 0)$ for the time series of $x_{1,2}(t)$ (top), maximum Lyapunov exponent λ_1 (middle), and transverse Lyapunov exponent $\lambda_\perp$ (bottom) as a function of feedback strength K and gap junction J. Here, the white region corresponding to $C(\tau = 0)$ represents the non-CCI region, i.e., the $x_{1,2}$ orbits are confined within the unilateral region ($a = 2.86$, $b = 10$, $\sigma = 0.6$, $N = 2$).

Fig. 5. The synchronization state ($C(0) \approx 1.0$) is maintained at $N \approx 10$. However, this state gradually becomes broken when $N \gtrsim 10$.

4. Discussion and Conclusions

In this study, we applied an RRO feedback controller that adjusts the existence range of chaotic orbits in a cubic map. It was confirmed that the attractor merging and CCI frequency can be controlled with this controller. Subsequently, it was determined that CCI synchronization is induced at an appropriate feedback strength in cubic maps coupled by a gap junction. In particular, the parameter region where a high-synchronization state arises is located at the border between the CCI feedback strength parameter region and the non-CCI region. It was determined that even if CCI synchronization occurs, the orbit of each element within the unilateral region does not synchronize. These characteristics of the induced CCI synchronization are largely maintained for large-scale coupled cubic maps.

The reasons for the enhancement of CCI synchronization at the edge between the CCI and non-CCI regions must be considered. Near the edge, attractor switching seldom occurs in the uncoupled case ($J = 0$). However, in the coupled case ($J > 0$), the influence of the attractor switching in the other oscillators leads to the breaking of the condition for the attractor to be separated into positive and negative regions. Therefore, the CCIs in the cubic maps synchronize with each other.

In conventional chaos control methods, chaotic states that could degrade system performance should be elimi-

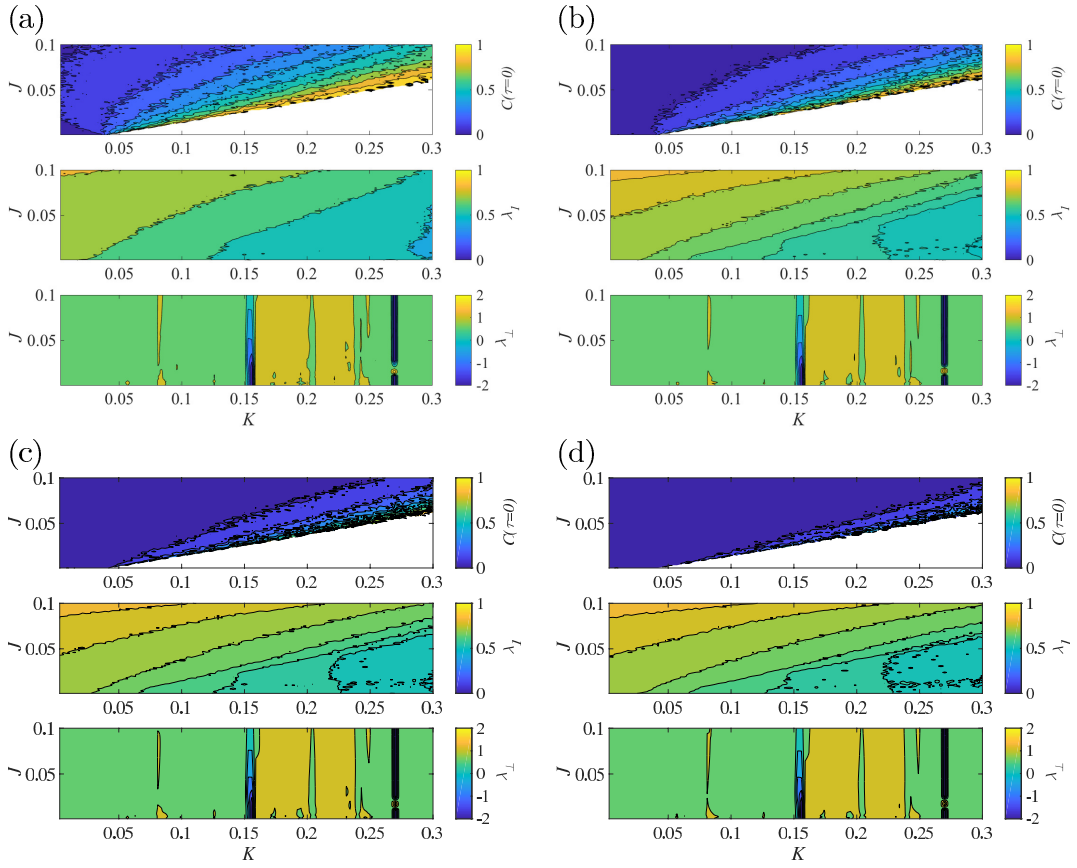

Fig. 4 Mean value of the correlation coefficient $C(\tau = 0)$ between the $x_i(t)$ and $x_j(t)$ time series $(i, j = 1, 2, \cdots N, i \neq j)$ for all pairs of cubic maps as a function of the gap junction J and the feedback strength K (top panels). Here, the white region represents the non-CCI region, i.e., the orbits of x_i are confined within the unilateral region. The maximum Lyapunov exponent λ_1 as a function of J and K (middle panels). The maximum transverse Lyapunov exponent $\lambda_\perp$ (bottom panels) as a function of J and K. (a) $N = 4$. (b) $N = 8$. (c) $N = 16$. (d) $N = 32$.

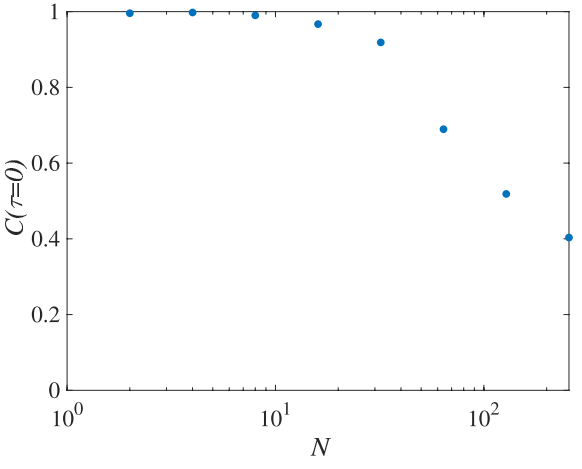

Fig. 5 Mean value of correlation coefficient $C(\tau = 0)$ for all pairs of cubic maps as a function of the size of the cubic map N.

nated, thereby achieving stable equilibrium and resulting in a transit to a periodic state through external perturbations such as OGY method and H_∞ method [38]–[41]. Indeed, a chaotic state transition to a periodic state in the high feedback strength region [25]. However, the chaotic state is maintained in the region where high CCI coherence arises, i.e., our proposed method induces an optimal chaotic state for CCI synchronization, instead of eliminating chaotic states.

Several nonlinear feedback controllers based on Lyapunov stability, active control and converse Lyapunov theories, realize chaos synchronization [31]–[34]. However, these methods do not permit an asynchronous state within each divided attractor. In contrast, our proposed method induces CCI synchronization, thus maintaining the asynchronous state within each divided attractor (corresponding to positive $\lambda_\perp$).

In regard to plausible alternative solutions for realizing CCI synchronization, our previously proposed feedback signal based on the utilization of the OGY method is a candidate [42]. This feedback signal was designed to induce attractor merging by reducing the instability of the orbit. However, after further evaluation of this solution, the OGY-based method did not exhibit the effect of inducing attractor merging to require CCI synchronization (see appendix). It is considered that the control mechanism of the OGY method is local, i.e., the effect of feedback cannot govern the wide

area and is restricted to neighboring regions of the unstable targets such as unstable equilibrium points. Therefore, CCI and attractor merging which includes wide-range behavior, cannot be controlled by the OGY based method.

With respect to the study of the application of coupled chaotic oscillators [43]–[45], Park et al. demonstrated that the movement patterns of snake-like robots are produced by chaotic coupled oscillators [45]. This oscillation exhibits chaotic itinerancy [46] which is the transition dynamics switching between the chaotic synchronized and desynchronized states. CCI synchronization and our proposed RRO feedback method may be used to generate movement patterns and control chaotic synchronized dynamics. However, for this application, the robustness and influence of CCI synchronization against the external perturbation, and the boundary condition for external environments must be considered. Therefore, as part of our future studies, these aspects will be evaluated.

Furthermore, we consider the process of applying RRO feedback to the general controlled chaotic system. In the cubic map case dealt with in this study, the peak of the map which induces attractor merging is initially specified by return map of the orbit. Secondly, feedback signals are designed with the effect of reducing the peak values. However, the cubic map is the simplest system with CCI. Therefore, to validate the applicability of this process, the design for RRO feedback must be considered in systems with a more complex map. Furthermore, in the case of continuous chaotic systems with CCI such as Chua's circuit and the Lorenz system, the RRO feedback for controlling attractor merging and CCI synchronization must be considered. Additionally, in this application stage, the comparison of applicability between a conventional feedback controller to achieve complete synchronization [31]–[34] and the RRO feedback method for CCI synchronization is an important subject. Therefore, as future works, we plan to evaluate these aspects.

In conclusion, the proposed nonlinear feedback controller can realize CCI synchronization, thus maintaining an asynchronous state within each divided attractor.

Acknowledgments

This work was supported by JSPS KAKENHI for Early-Career Scientists Grant Number 18K18124 (SN) and Grant-in-Aid for Scientific Research (C) Grant Number 18K11450 (TY).

References

[1] Q. Wang, Z. Duan, M. Perc, and G. Chen, "Synchronization transitions on small-world neuronal networks: Effects of information transmission delay and rewiring probability," EPL (Europhysics Letters), vol.83, no.5, p.50008, 2008.
[2] Q. Wang, M. Perc, Z. Duan, and G. Chen, "Synchronization transitions on scale-free neuronal networks due to finite information transmission delays," Phys. Rev. E, vol.80, no.2, p.026206, 2009.
[3] Q. Wang, G. Chen, and M. Perc, "Synchronous bursts on scale-free neuronal networks with attractive and repulsive coupling," PLoS ONE, vol.6, no.1, p.e15851, 2011.
[4] S. Majhi, M. Perc, and D. Ghosh, "Chimera states in uncoupled neurons induced by a multilayer structure," Scientific Reports, vol.6, 2016.
[5] J. Hizanidis, N.E. Kouvaris, G. Zamora-López, A. Díaz-Guilera, and C.G. Antonopoulos, "Chimera-like states in modular neural networks," Scientific Reports, vol.6, p.19845, 2016.
[6] B.K. Bera, D. Ghosh, and T. Banerjee, "Imperfect traveling chimera states induced by local synaptic gradient coupling," Phys. Rev. E, vol.94, no.1, p.012215, 2016.
[7] R. Benzi, A. Sutera, and A. Vulpiani, "The mechanism of stochastic resonance," J. Phys. A: Math. Gen., vol.14, no.11, pp.L453–L457, 1981.
[8] F. Moss and K. Wiesenfeld, "The benefits of background noise," Sci. Am., vol.273, no.2, pp.66–69, 1995.
[9] L. Gammaitoni, P. Hänggi, P. Jung, and F. Marchesoni, "Stochastic resonance," Rev. Mod. Phys., vol.70, no.1, pp.223–287, 1998.
[10] A. Pikovsky, M. Rosenblum, and J. Kurths, Synchronization: A Universal Concept in Nonlinear Sciences, Cambridge University Press, 2003.
[11] V.S. Anishchenko, V. Astakhov, A. Neiman, T. Vadivasova, and L. Schimansky-Geier, Nonlinear Dynamics of Chaotic and Stochastic Systems: Tutorial and Modern Developments, Springer Science & Business Media, 2007.
[12] T. Carroll and L. Pecora, "Stochastic resonance and crises," Phys. Rev. Lett., vol.70, no.5, pp.576–579, 1993.
[13] T. Carroll and L. Pecora, "Stochastic resonance as a crisis in a period-doubled circuit," Phys. Rev. E, vol.47, no.6, pp.3941–3949, 1993.
[14] A. Crisanti, M. Falcioni, G. Paladin, and A. Vulpiani, "Stochastic resonance in deterministic chaotic systems," J. Phys. A: Math. Gen., vol.27, no.17, pp.597–603, 1994.
[15] G. Nicolis, C. Nicolis, and D. McKernan, "Stochastic resonance in chaotic dynamics," J. Stat. Phys., vol.70, no.1-2, pp.125–139, 1993.
[16] S. Sinha and B.K. Chakrabarti, "Deterministic stochastic resonance in a piecewise linear chaotic map," Phys. Rev. E, vol.58, no.6, pp.8009–8012, 1998.
[17] H. Nishimura, N. Katada, and K. Aihara, "Coherent response in a chaotic neural network," Neural Process. Lett., vol.12, no.1, pp.49–58, 2000.
[18] S. Nobukawa, H. Nishimura, and N. Katada, "Chaotic resonance by chaotic attractors merging in discrete cubic map and chaotic neural network," IEICE Trans. A, vol.95, no.4, pp.357–366, 2012.
[19] N. Schweighofer, E.J. Lang, and M. Kawato, "Role of the olivo-cerebellar complex in motor learning and control," Front. Neural Circuits, vol.7, no.94, pp.10–3389, 2013.
[20] I.T. Tokuda, C.E. Han, K. Aihara, M. Kawato, and N. Schweighofer, "The role of chaotic resonance in cerebellar learning," Neural Networks, vol.23, no.7, pp.836–842, 2010.
[21] S. Nobukawa, H. Nishimura, T. Yamanishi, and J.Q. Liu, "Analysis of chaotic resonance in izhikevich neuron model," PloS ONE, vol.10, no.9, p.e0138919, 2015.
[22] S. Nobukawa, H. Nishimura, and T. Yamanishi, "Chaotic resonance in typical routes to chaos in the izhikevich neuron model," Scientific Reports, vol.7, p.1331, 2017.
[23] Y. Kurita, M. Shinohara, and J. Ueda, "Wearable sensorimotor enhancer for fingertip based on stochastic resonance effect," IEEE Trans. Human-Mach. Syst., vol.43, no.3, pp.333–337, 2013.
[24] Y. Kurita, Y. Sueda, T. Ishikawa, M. Hattori, H. Sawada, H. Egi, H. Ohdan, J. Ueda, and T. Tsuji, "Surgical grasping forceps with enhanced sensorimotor capability via the stochastic resonance effect," IEEE/ASME Trans. Mechatronics, vol.21, no.6, pp.2624–2634, 2016.
[25] S. Nobukawa, H. Nishimura, T. Yamanishi, and H. Doho, "Controlling chaotic resonance in systems with chaos-chaos intermittency using external feedback," IEICE Trans. Fundamentals, vol.E101-A, no.11, pp.1900–1906, Nov. 2018.
[26] H. Fujisaka and T. Yamada, "Stability theory of synchronized motion in coupled-oscillator systems," Prog. Theor. Phys., vol.69, no.1,

pp.32–47, 1983.
[27] A. Pikovsky, "On the interaction of strange attractors," Zeitschrift für Physik B Condensed Matter, vol.55, no.2, pp.149–154, 1984.
[28] L.M. Pecora and T.L. Carroll, "Synchronization in chaotic systems," Phys. Rev. Lett., vol.64, no.8, pp.821–824, 1990.
[29] M.G. Rosenblum, A.S. Pikovsky, and J. Kurths, "Phase synchronization of chaotic oscillators," Phys. Rev. Lett., vol.76, no.11, pp.1804–1807, 1996.
[30] N.F. Rulkov, M.M. Sushchik, L.S. Tsimring, and H.D. Abarbanel, "Generalized synchronization of chaos in directionally coupled chaotic systems," Phys. Rev. E, vol.51, no.2, pp.980–994, 1995.
[31] L. Huang, R. Feng, and M. Wang, "Synchronization of chaotic systems via nonlinear control," Phys. Lett. A, vol.320, no.4, pp.271–275, 2004.
[32] H.K. Chen, "Global chaos synchronization of new chaotic systems via nonlinear control," Chaos, Solitons & Fractals, vol.23, no.4, pp.1245–1251, 2005.
[33] M. Yassen, "Chaos synchronization between two different chaotic systems using active control," Chaos, Solitons & Fractals, vol.23, no.1, pp.131–140, 2005.
[34] H.H. Chen, G.J. Sheu, Y.L. Lin, and C.S. Chen, "Chaos synchronization between two different chaotic systems via nonlinear feedback control," Nonlinear Analysis: Theory, Methods & Applications, vol.70, no.12, pp.4393–4401, 2009.
[35] S. Nobukawa, H. Nishimura, T. Yamanishi, and H. Doho, "Induced synchronization of chaos-chaos intermittency in coupled cubic maps by external feedback signals," 2018 5th International Conference on Control, Decision and Information Technologies (CoDIT), pp.64–68, IEEE, 2018.
[36] T.S. Parker and L. Chua, Practical Numerical Algorithms for Chaotic Systems, Springer Science & Business Media, 2012.
[37] A. Dabrowski, "The largest transversal lyapunov exponent and master stability function from the perturbation vector and its derivative dot product (TLEVDP)," Nonlinear Dynam., vol.69, no.3, pp.1225–1235, 2012.
[38] E. Ott, C. Grebogi, and J.A. Yorke, "Controlling chaos," Phys. Rev. Lett., vol.64, no.11, pp.1196–1199, 1990.
[39] K. Pyragas, "Continuous control of chaos by self-controlling feedback," Phys. Lett. A, vol.170, no.6, pp.421–428, 1992.
[40] H. Nakajima, "On analytical properties of delayed feedback control of chaos," Phys. Lett. A, vol.232, no.3-4, pp.207–210, 1997.
[41] W. Jiang, Q. Guo-Dong, and D. Bin, "H^{∞} variable universe adaptive fuzzy control for chaotic system," Chaos, Solitons & Fractals, vol.24, no.4, pp.1075–1086, 2005.
[42] S. Nobukawa, H. Nishimura, and T. Yamanishi, "Controlling method for attractor merged chaotic resonance by external feedback," Proc. SICE Annual Conference (SICE2017), pp.684–688, IEEE, 2017.
[43] G. Ren, W. Chen, S. Dasgupta, C. Kolodziejski, F. Wörgötter, and P. Manoonpong, "Multiple chaotic central pattern generators with learning for legged locomotion and malfunction compensation," Information Sciences, vol.294, pp.666–682, 2015.
[44] J. Fan, Y. Zhang, H. Jin, X. Wang, D. Bie, J. Zhao, and Y. Zhu, "Chaotic cpg based locomotion control for modular self-reconfigurable robot," J. Bionic Eng., vol.13, no.1, pp.30–38, 2016.
[45] J. Park, H. Mori, Y. Okuyama, and M. Asada, "Chaotic itinerancy within the coupled dynamics between a physical body and neural oscillator networks," PloS ONE, vol.12, no.8, p.e0182518, 2017.
[46] K. Kaneko and I. Tsuda, Complex Systems: Chaos and Beyond: A Constructive Approach with Applications in Life Sciences, Springer Science & Business Media, 2011.

Appendix:

In our previous study [42], we introduced the one-dimensional cubic map model with external feedback $u(x)$ based on the OGY method. This system is given by:

$$x(t+1) = (ax(t) - x(t)^3)\exp(-x(t)^2/b) + Ku(x(t)), \quad (\text{A}\cdot 1)$$

$$u(x(t)) = K^+(x)(x^+ - x(t)) + K^-(x)(x^- - x(t)), \quad (\text{A}\cdot 2)$$

where K represents the amplitude related to the intensity of the feedback control. $x^{\pm}$ are two symmetric (positive and negative) nearest neighbor equilibrium points around $x(t) = 0$. Here, the values of $x^{\pm}$ are determined by numerically solving the equation $x - (ax - x^3)\exp(-x^2/b) = 0$. In our previous study, we set the targets for the OGY method to $x^{\pm}$ and added the feedback terms of $(x^+ - x(t))$ and $(x^- - x(t))$ related to the distance of the equilibrium points. To decrease the instability for unstable equilibrium points in the region where $x(t)$, i.e., x^+ if $x(t) > 0$ or x^- if $x(t) < 0$, we adopted

$$K^+(x) = \exp(-\frac{(x(t) - x^+)^2}{2\sigma^2}), \quad (\text{A}\cdot 3)$$

$$K^-(x) = \exp(-\frac{(x(t) - x^-)^2}{2\sigma^2}), \quad (\text{A}\cdot 4)$$

as gain functions for $(x^+ - x(t))$ and $(x^- - x(t))$, respectively. Here, σ represents the area of influence of $u(t)$. Thus, the influence of the gain function corresponding to the chaotic attractor comprising $x(t)$ increases in comparison with the other gain function. We assume that chaos–chaos intermittency arises when the system state of $x(t)$ deviates from the equilibrium points significantly ($x(t) \approx 0$). Therefore, increasing the residence time around $x^{\pm}$ diminishes the frequency of chaos–chaos intermittency. In this study, we exhaustively checked whether the previously proposed method in Ref. [42] can control attractor merging by stabilizing unstable equilibrium points. We confirmed that control $u(x(t))$ does not vanish at the region with a sufficiently large distance from $x^{\pm}$ under the condition $\sigma = 1.4$ in Ref. [42]. However, in the OGY method, feedback control only activates near the target equilibrium points. Therefore, the setting for $\sigma = 1.4$ is too large for the OGY method.

We reduced the σ value in Eqs. (A·3) and (A·4). For small values of σ ($\sigma = 0.1$), where $u(x(t))$ only activates near $x^{\pm}$, we did not observe merging of the chaotic attractor, as shown in Fig. A·1(b). Note that Fig. A·1(a) shows the result for a large value of $\sigma(= 1.4)$ (corresponding to the result of Ref. [42]). Therefore, we conclude that stabilization of unstable equilibrium points $x^{\pm}$, that is, the mechanism of the OGY method, does not contribute to attractor merging.

Subsequently, we evaluated the maps of Eqs. (A·1)–(A·4) for the cases of $K = 0.5$ and 0 ($\sigma = 1.4$ corresponding to Fig. A·1(a)), as shown in Fig. A·2. We confirmed that this feedback has the effect of reducing the local maximum and minimum values of the map at $x \approx \pm 0.916$, similar to RRO feedback [25]. Therefore, the attractor merging observed in Fig. A·1(a) are induced by the mechanism for RRO feedback, not the OGY method.

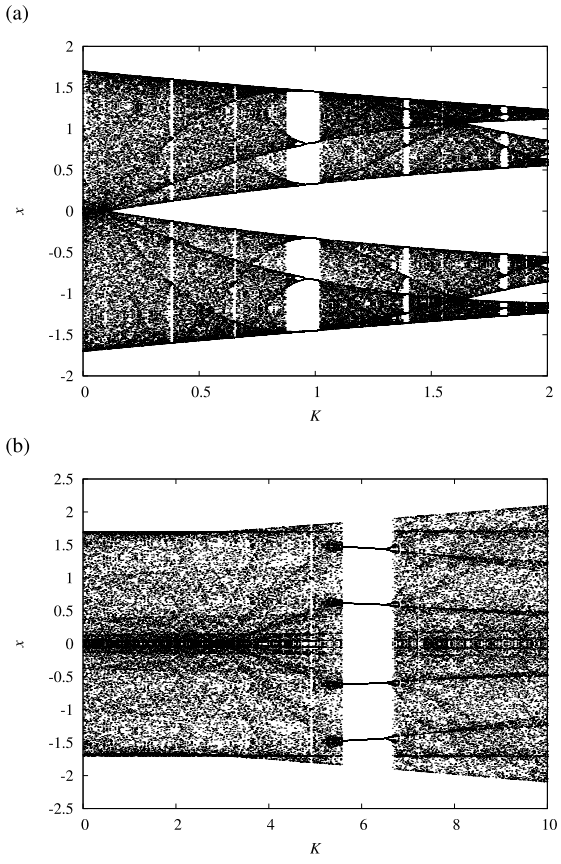

Fig. A · 1 Bifurcation diagram of $x(t)$ as function of K in Eqs. (A · 1)–(A · 4) ($b = 10$, $A = 0$, $a = 2.86$, and $x^{\pm} \approx \pm 1.29$) (a) $\sigma = 1.4$ case corresponding to the parameter set in our previous work [42]. (b) $\sigma = 0.1$ case.

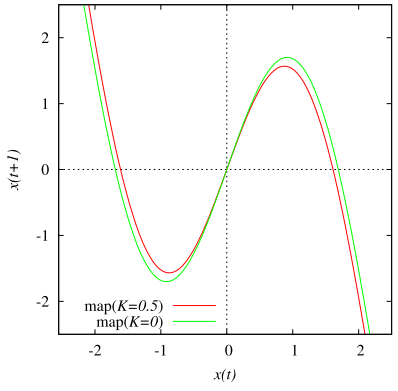

Fig. A · 2 Map of Eqs. (A · 1)–(A · 4) for $\sigma = 1.4$ case corresponding the parameter set in our previous investigation ($b = 10$, $A = 0$, $a = 2.86$, and $x^{\pm} \approx \pm 1.29$) [42].

Sou Nobukawa graduated from the Department of Physics and Earth Sciences University of Ryukyus in 2006, completed the doctoral program at University of Hyogo, and received the Ph.D. degree in 2013. He is an Associate Professor in the Department of Computer Science, Chiba Institute of Technology. His research interests include chaos/bifurcation and neural networks. He is a member of IEEE, INNS, IEICE, IPSJ, SICE, ISCIE, and others, and was awarded the SICE encouraging prize in 2016.

Haruhiko Nishimura graduated from the Department of Physics, Shizuoka University in 1980, completed the doctoral program at Kobe University, and received the Ph.D. degree in 1985. He is currently a Professor in the Graduate School of Applied Informatics, University of Hyogo. His research interests include intelligent systems science based on several architectures such as neural networks and complex systems. He is also presently engaged in research in biomedical, healthcare, and high confidence sciences. He is a member of the IEEE, IEICE, IPSJ, ISCIE, JNNS, and others, and was awarded ISCIE paper prize in 2001 and JSKE paper prize in 2010.

Teruya Yamanishi received the Master's degree in education of science from Kobe University in 1991, and the Ph.D. degree in physics from Kobe University in 1994. He is a Professor at Fukui University of Technology, where he studies mathematical information science for the brain, and develops optimization tools for behavior of autonomous robots.

Hirotaka Doho graduated from the Faculty of School of Education, Hiroshima University in 1985, completed the Master's program at Hyogo University of Education, and received the Master's degree in 2000. He is a Professor in the Faculty of Education, Kochi University. His research interests include nonlinear dynamics of neural networks.